

EuPdIn₂, YbPdIn₂, and YbAuIn₂: Syntheses, Structures, and Properties of New Intermetallic Compounds with Ordered Re₃B-Type Structure

Yaroslav V. Galadzhun,^[a] Rolf-Dieter Hoffmann,^[a] Gunter Kotzyba,^[a] Bernd Künnen,^[a] and Rainer Pöttgen^{*[a]}

Keywords: Europium / Ytterbium / Indium / Intermetallic compounds / Ferromagnetism

The new compounds EuPdIn₂ (**1**), YbPdIn₂ (**2**), and YbAuIn₂ (**3**) have been synthesized by high-frequency melting of the elements in sealed tantalum tubes and subsequent annealing at about 900 K. Their crystal structures have been determined by single-crystal X-ray diffraction techniques. Compounds **1**, **2**, and **3** crystallize with the MgCuAl₂-type structure (space group *Cmcm*), a ternary ordered version of the Re₃B type. Structural elements in these compounds are transition metal centered trigonal prisms made up of the rare earth and indium atoms. The transition metal (T) and indium atoms form a three-dimensionally infinite [TIn₂] polyanionic network in which the large rare earth metal atoms occupy one-dimensional pentagonal tubes. A semiempirical band

structure calculation on **1** reveals a non-vanishing density-of-states (DOS) at the Fermi level. The strongest bonding interactions are found for the In–In and Pd–In contacts; the Eu–Pd and Eu–In interactions are much weaker. Magnetic investigations indicate divalent character of the ytterbium atoms in **2**, showing negative susceptibilities below room temperature. Compound **1** exhibits Curie–Weiss behavior above 50 K with an experimental magnetic moment of 7.8(1) μ_B , thus indicating divalent europium. Ferromagnetic ordering was observed at $T_C = 14.5(5)$ K, with a saturation moment of 6.8(1) μ_B /Eu at 5.5 T and 4 K, as determined from magnetization measurements. Compounds **1** and **2** are found to be metallic conductors.

Introduction

The ternary systems rare earth (RE)/transition metal (T)/indium have been extensively studied in the course of phase analytical investigations and crystal structure determinations.^{[1][2]} The structures of a multitude of ternary compounds of this type are governed by two- or three-dimensionally infinite polyanions made up of the transition metal and indium atoms. The rare earth metal atoms, as the most electropositive component, are located within cavities or channels of the [T_xIn_y] networks.

Investigations to date have mainly been focused on compounds with trivalent rare earth metal atoms, whereas relatively little information is available on compounds with alkaline earth metals, europium, or ytterbium as the electropositive component. A reason for this is most certainly the more complicated synthesis conditions required for the latter systems.

Most of the compounds RE_xT_yIn_z with trivalent rare earth metals are easily accessible by means of arc-melting of the elemental components. However, due to the low boiling temperatures of the alkaline earth metals, europium, and ytterbium, such a synthetic approach employing arc-melting techniques would invariably result in large weight losses due to evaporation of these volatile metals. We have now succeeded in overcoming these experimental difficulties by modifying the synthesis conditions: (i) alkaline earth compounds such as CaAuIn^[3] can be prepared in a quantitative manner by reacting the elements in glassy carbon crucibles

in a novel, water-cooled sample chamber in a high-frequency furnace^[3]; (ii) compounds with europium and ytterbium as the electropositive component are best prepared by high-frequency melting of the elements in sealed tantalum containers in a water-cooled quartz glass apparatus. The latter technique was first employed in syntheses of the stanides YbPtSn and Yb₂Pt₃Sn₅.^[4] We have now extended these syntheses to indium compounds and have succeeded in preparing the new compounds EuPdIn₂, YbPdIn₂, and YbAuIn₂ reported herein. The present paper also deals with structure determinations and an analysis of the chemical bonding in these systems, as well as a detailed investigation of their physical properties.

Results and Discussion

Crystal Structures and Chemical Bonding of EuPdIn₂, YbPdIn₂, and YbAuIn₂

The new intermetallic compounds **1**, **2**, and **3** each adopt the MgCuAl₂-type structure,^[5] a ternary ordered version of the Re₃B type.^[6] As a representative example, a projection of the EuPdIn₂ structure is presented in Figure 1. From a geometrical point of view, the indium and europium atoms in **1** form slightly distorted trigonal prisms (every other prism is shifted by half the translation period *a*), and these prisms have palladium atoms at their centers.

The Pd–In distances (Table 1) of 277 and 284 pm in **1** agree well with the sum of Pauling single bond radii of 278 pm.^[7] Similar distances have also been observed in the distorted tetrahedral [PdIn] polyanion in equiatomic EuPdIn (282 and 283 pm).^[8] Due to the twofold higher indium con-

^[a] Anorganisch-Chemisches Institut, Universität Münster, Wilhelm-Klemm-Straße 8, D-48149 Münster, Germany
E-mail: pottgen@uni-muenster.de

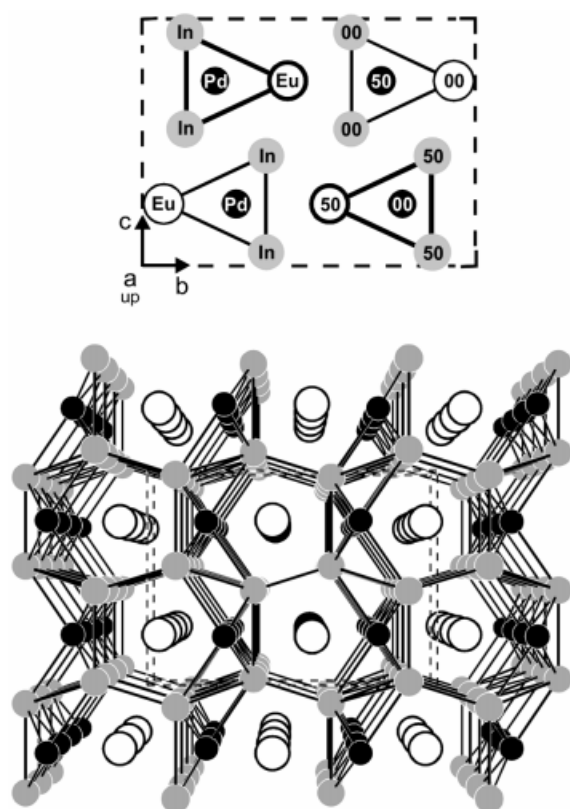


Figure 1. Projection (upper part) of the crystal structure of EuPdIn_2 onto the yz plane, emphasizing the topological arrangement of palladium-centered trigonal prisms made up of europium and indium atoms (black filled, open, and grey filled circles, respectively). The height of the atoms is given in the upper part in hundredths. In the lower part, a perspective view of the same orientation is depicted, showing an outline of the polyanionic network of palladium and indium atoms

tent, **1** has a higher degree of linkage of indium atoms, four contacts at 308 ($1\times$) and 324 pm ($3\times$), as compared to EuPdIn , which has one contact at 326 pm. The indium atoms together with the palladium atoms form a three-dimensionally infinite $[\text{PdIn}_2]$ polyanion, in which the europium atoms occupy distorted pentagonal channels as outlined in Figure 1. Nevertheless, there are still quite short Eu–Pd (297 and 323 pm) and Eu–In (341 pm) contacts, indicating a weak linkage of the europium atoms to the pentagonal channels. This rough assessment of the chemical bonding in **1**, made by considering only the interatomic distances, is nicely supported by the results of an extended Hückel calculation, which is discussed in detail below.

The density-of-states (DOS) for **1** is presented in Figure 2. In the DOS, the palladium contribution extends mainly from -10 eV to -8 eV, while the indium contributions extend over the whole valence region. The non-vanishing DOS at the Fermi level is in agreement with the metallic behavior discussed below. A Mulliken population analysis reveals the net charges Eu: $+1.78$, Pd: -1.16 , In: -0.31 , with the palladium atoms as the most electronegative component of **1**, in good agreement with Pearson's absolute electronegativities^[9] of 4.45 and 3.10 eV for palladium and indium, respectively. Unfortunately, no value for the abso-

Table 1. Interatomic distances (pm) in the structures of EuPdIn_2 , YbPdIn_2 , and YbAuIn_2 ; all distances of the first coordination sphere are listed; standard deviations are all 0.2 pm or less

EuPdIn_2			YbPdIn_2			YbAuIn_2		
Eu:	1	Pd 296.9	Yb:	1	Pd 292.8	Yb:	1	Au 308.5
	2	Pd 323.2		2	Pd 314.6		2	Au 323.6
	2	In 304.5		4	In 334.2		4	In 328.2
	4	In 341.2		2	In 336.0		2	In 345.7
	4	In 353.5		4	In 346.3		4	In 355.1
	2	Eu 414.9		2	Yb 413.2		2	Au 404.7
	2	Pd 425.0		2	Pd 420.1		2	Yb 411.2
	2	Eu 453.6		2	Yb 444.3		2	Yb 455.9
Pd:	2	In 277.4	Pd:	2	In 276.1	Au:	2	In 281.2
	4	In 283.7		4	In 280.5		4	In 285.0
	1	Eu 296.9		1	Yb 292.8		1	Yb 308.5
	2	Eu 323.2		2	Yb 314.6		2	Yb 323.6
	2	Eu 425.0		2	Yb 420.1		2	Yb 404.7
In:	1	Pd 277.4	In:	1	Pd 276.1	In:	1	Au 281.2
	2	Pd 283.7		2	Pd 280.5		2	Au 285.0
	1	In 307.7		1	In 307.0		1	In 300.7
	2	In 323.6		1	In 308.3		1	In 301.0
	1	In 323.9		2	In 322.6		2	Yb 328.2
	1	Eu 340.5		2	Yb 334.2		2	In 344.9
	2	Eu 341.2		1	Yb 336.0		1	Yb 345.7
	2	Eu 353.5		2	Yb 346.3		2	Yb 355.1

lute electronegativity of europium is listed by Pearson.^[9] Since europium exhibits chemical behavior similar to that of the alkaline earth metals calcium ($\chi = 2.2$ eV) and strontium ($\chi = 2.0$ eV), we assume a comparably low χ value for this rare earth element.

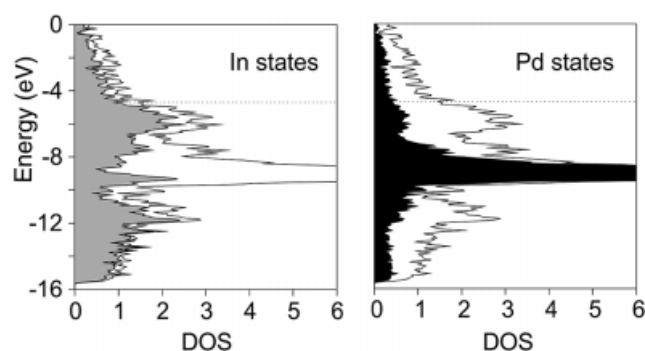


Figure 2. Density-of-states (DOS) for EuPdIn_2 with the indium and palladium contributions emphasized in grey and black, respectively; the Fermi level E_F is drawn as a dotted line

The In–In distances in **1** are all shorter than in the tetragonal body-centered structure of elemental indium ($a = 325.2$ pm, $c = 494.7$ pm^[10]), where each indium atom has four nearest neighbors at 325.2 pm and eight further neighbors at 337.7 pm. The strong bonding character of the In–In contacts in **1** is reflected by the highest overlap population (OP) of $+0.522$ (Figure 3). The close Pd–In contacts (277–284 pm) also show a significant overlap population of $+0.390$.

In contrast, the Eu–Pd (OP $+0.022$) and Eu–In (OP $+0.039$) overlap populations are much smaller, in agreement with our description in terms of a polyanionic $[\text{PdIn}_2]$ network. Bonding between the palladium and indium atoms within the network is much stronger than the interactions of the europium atoms in the distorted pentagonal

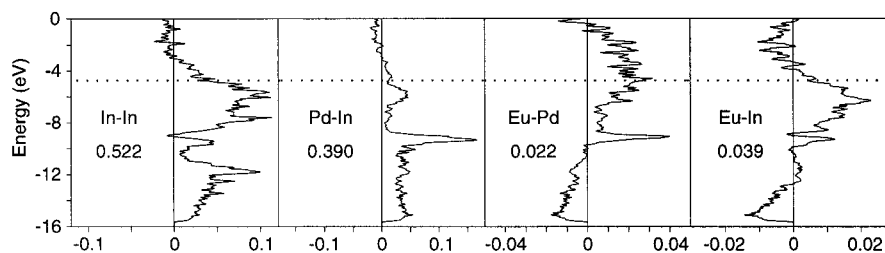


Figure 3. Chemical bonding from semiempirical crystal orbital overlap populations (COOP) for various bonding contributions in EuPdIn_2 ; the numbers represent the integrated values of the overlap population per bond, integrated up to the Fermi level (dotted line)

channels with the network. Chemical bonding in isotypic **2** and **3** is most likely analogous to that in **1**, with the palladium and gold atoms carrying most of the negative charge.

Magnetic Properties

The magnetic susceptibility of **2** as a function of temperature is plotted in Figure 4. Over the whole temperature range investigated the susceptibility of **2** is negative and has a value of $-6.2(2) \cdot 10^{-9} \text{ m}^3/\text{mol}$ at room temperature. At first sight, these findings appear to suggest diamagnetism. This, however, would seem to be at variance with the metallic behavior discussed below. In fact, the core diamagnetism of **2** dominates compared to the much weaker Pauli contribution of the conduction electrons, thus resulting in slightly negative susceptibilities. Similar magnetic behavior has recently been observed for the indium-rich binary compounds TIn_3 ($\text{T} = \text{Co}, \text{Ru}, \text{Rh}, \text{Ir}$)^{[11][12]} and the isotypic calcium compounds CaTIn_2 ($\text{T} = \text{Pd}, \text{Pt}, \text{Au}$).^[13] A reasonable correction for the core diamagnetism, however, is difficult to perform, since no reliable increments for ytterbium, palladium, and indium are available in the literature. Rough estimates for the diamagnetic contributions in TIn_3 ($\text{T} = \text{Co}, \text{Rh}, \text{Ir}$) and CaAuIn_2 are reported in ref.^[12] and ref.^[13]

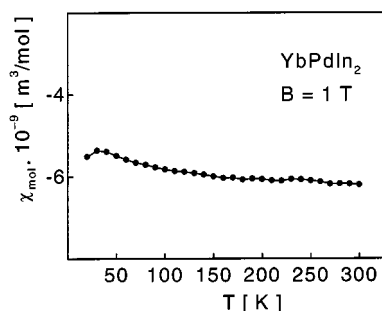


Figure 4. Temperature dependence of the magnetic susceptibility of **2**, measured at a magnetic flux density of 1 T

Compound **1** shows Curie–Weiss behavior above 50 K (Figure 5). An evaluation of the data above 50 K resulted in an experimental magnetic moment of $7.8(1) \mu_{\text{B}}/\text{Eu}$ and a paramagnetic Curie temperature of $\theta = 22(1) \text{ K}$. Ferromagnetic ordering of the europium atoms was detected at low temperatures (Figure 6). The precise Curie temperature of $T_{\text{C}} = 14.5(5) \text{ K}$ was determined from the derivative $d\chi/dT$ of a kink-point measurement (inset of Figure 6) at a mag-

netic flux density of 0.002 T. The derivative additionally revealed a further feature at $12.5(2) \text{ K}$, probably due to a very small impurity of EuPdIn ,^[8] which has a Néel temperature of 13.0 K .^{[8][14]} Nevertheless, our Guinier powder pattern revealed a single-phase material. The magnetization curve at 50 K (Figure 7) was linear, as expected for a paramagnet. At 4 K, we observed a strong increase of the magnetization, even at very low field strengths. The magnetization curve tends to saturation at just 1 T and shows only a small hysteresis with negligible coercivity and remanent magnetization. On the basis of these features, **1** can clearly be classified as a soft ferromagnet. At the highest obtainable magnetic field of 5.5 T, the saturation magnetization amounts to $\mu_{\text{SM}(\text{exp})} = 6.8(1) \mu_{\text{B}}/\text{Eu}$, in good agreement with the maximum possible value of $\mu_{\text{SM}(\text{calcd})} = 7.0 \mu_{\text{B}}/\text{Eu}$, indicating an almost fully parallel spin alignment.

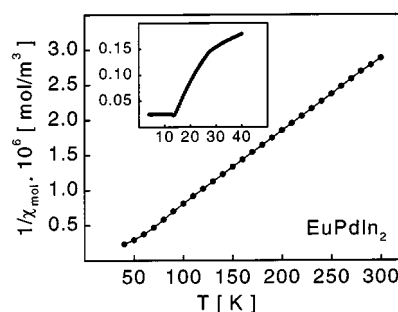


Figure 5. Temperature dependence of the reciprocal susceptibility of **1** determined at a magnetic flux density of 2 T; the low-temperature behaviour is shown in the inset

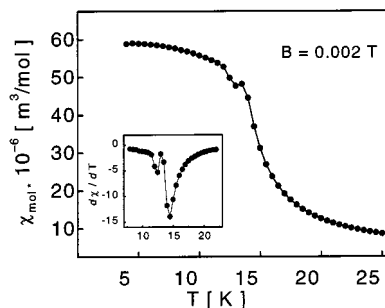


Figure 6. Low-temperature susceptibility (field-cooling mode) of **1** at 0.002 T (kink-point measurement). The inset shows the derivative $d\chi/dT$, which has a sharp peak at $T_{\text{C}} = 14.5(2) \text{ K}$. The second anomaly at $12.5(5) \text{ K}$ is most likely due to a minor impurity of metamagnetic EuPdIn , which becomes magnetically ordered at 13.0 K ^{[8][14]}

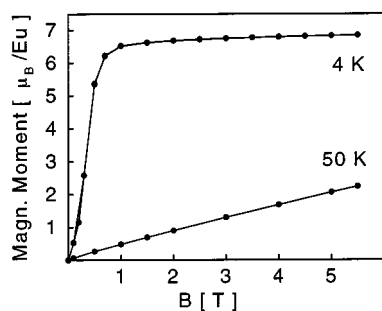


Figure 7. Magnetic moment vs. external magnetic flux density, B_{ext} , of **1** at 50 and 4 K

Electrical Conductivity

The temperature dependences of the specific resistivities of **1** and **2** are plotted in Figure 8. The specific resistivities of both compounds decrease with decreasing temperature, as is of course typical for metallic conduction. At room temperature, the values amount to $34 \pm 5 \mu\Omega\text{cm}$ for **1** and $27 \pm 5 \mu\Omega\text{cm}$ for **2**, indicating that both compounds are relatively good metallic conductors. The large margins of error account for the different values obtained with a series of samples. At about 4 K, the specific resistivities of **1** and **2** fall to 68% and 59% of their room temperature values, respectively. While no anomaly can be detected in the temperature dependence of ρ in the case of **2**, a very small drop is seen for **1** at the Curie temperature. This most likely results from a freezing of spin-disorder scattering below T_C .

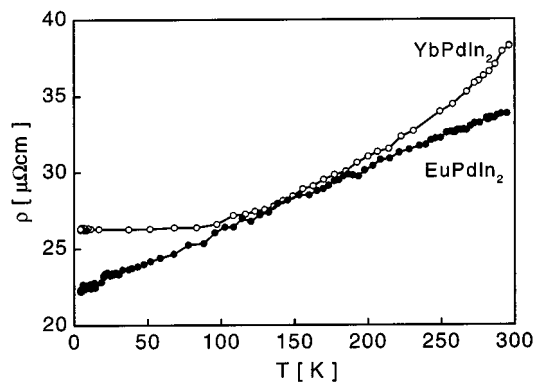


Figure 8. Temperature dependence of the specific resistivities of **1** and **2**

Experimental Section

Syntheses: Starting materials were europium ingots (Johnson Matthey), ytterbium rods (Kelpin), palladium powder (Degussa), gold wire (Degussa, \varnothing 1 mm), and indium “teardrops” (Johnson Matthey), all with stated purities in excess of 99.9%. The moisture-sensitive ingots of europium and ytterbium were stored in vacuo prior to carrying out the reactions. The elemental components were mixed in the ideal 1:1:2 atomic ratio and sealed in tantalum tubes under an argon pressure of about 800 mbar. The argon was purified by passage over silica gel, molecular sieves, and titanium sponge (900 K). The tantalum tubes were then annealed in a novel, water-cooled sample chamber^[4] in a high-frequency furnace (Kontron,

Roto-Melt). In a first step, the tubes were heated with the maximum power output of the high-frequency generator. The occurrence of the strongly exothermic reactions was evident from a heat flash that lasted for about two seconds. The annealing temperature was then lowered to about 1000–1100 K for one minute and then raised to the maximum possible once more. Subsequently, the tubes were annealed for 30 min at about 800–900 K. The reactions resulted in polycrystalline products, which could easily be separated from the tantalum tubes. No tantalum contamination could be detected by EDX analyses. While **1** and **2** were obtained as single-phase products, **3** was accompanied by very small amounts of YbAuIn^[15] (Fe₂P type) and elemental indium. Products **1**, **2**, and **3** are grey in compact form, while single crystals are silvery with a metallic lustre. Powders and compact pieces of these intermetallic compounds are stable in air; no deterioration was observed over a period of several weeks.

X-ray Investigations: Guinier powder patterns of all samples were recorded with Cu- $K_{\alpha 1}$ radiation using α -quartz ($a = 491.30$ pm, $c = 540.46$ pm) as an internal standard. The indexing of the patterns was facilitated by comparison of the observed patterns with calculated ones,^[16] taking the atomic positions from the structure refinements. Single-crystal intensity data were collected at room temperature using a four-circle diffractometer (Enraf-Nonius, CAD4) with graphite-monochromated Mo- K_{α} radiation ($\lambda = 71.073$ pm) and a scintillation counter with pulse height discrimination. The scans were taken in the ω -2 θ mode. Absorption corrections were applied on the basis of Ψ -scan data. Single crystals of **1**, **2**, and **3** were isolated from the samples by mechanical fragmentation. Buerger precession photographs of the three compounds (reciprocal layers $hk0$ and $0kl$) showed C-centered orthorhombic lattices with symmetry mmm . The systematic extinctions (hkl only observed for $h + k = 2n$; $0kl$ only with $k = 2n$) led to the space groups $Cmcm$ (No. 63) and $Cmc2_1$ (No. 36), of which the centrosymmetric group was found to be the correct one during the structure refinements. All relevant crystallographic data and experimental details are listed in Table 2.

The starting atomic parameters were obtained by direct methods using an automatic interpretation as implemented in SHELXS-86.^[17] The structures were subsequently refined with anisotropic displacement parameters for all atoms using SHELXL-97 (full-matrix least-squares on F^2).^[18] Final difference Fourier syntheses were flat and revealed no significant residual peaks. The results of the refinements are summarized in Table 2. Atomic coordinates and interatomic distances are listed in Tables 3 and 1, respectively. Further details of the crystal structure determinations may be obtained from the Fachinformationszentrum Karlsruhe, D-76344 Eggenstein-Leopoldshafen (Germany), by quoting the registry numbers CSD-410438 (EuPdIn₂), CSD-410437 (YbPdIn₂), and CSD-410436 (YbAuIn₂).

Electronic Structure Calculations: Semiempirical band structure calculations were based on an extended Hückel Hamiltonian,^{[19][20]} where off-site Hamiltonian matrix elements were evaluated according to the weighted Wolfsberg–Helmholz formula,^[21] minimizing counter-intuitive orbital mixing. The extended Hückel parameters used for the calculations were taken from refs.^{[22][23]} (ξ orbital exponents in parentheses): Eu 6s –4.663 eV (1.345) and Eu 6p –3.403 eV (1.231); Pd 5s –9.224 eV (1.658), Pd 5p –3.279 eV (1.182), and Pd 4d –8.985 eV, $\xi_1 = 3.746$, $c_1 = 0.815$, $\xi_2 = 1.501$, $c_2 = 0.338$; In 5s –10.79 eV (2.02) and In 6p –5.35 eV (1.47). The eigenvalue problem was solved in reciprocal space at 144 k points within the irreducible wedge of the Brillouin zone by using the YAEHMOP code.^[24]

Table 2. Crystal data, details of the data collections, and structure refinements of EuPdIn₂ (1), YbPdIn₂ (2), and YbAuIn₂ (3) (all with space group *Cmcm* and *Z* = 4)

	EuPdIn ₂	YbPdIn ₂	YbAuIn ₂
Empirical formula	EuPdIn ₂	YbPdIn ₂	YbAuIn ₂
Molar mass	488.0 g/mol	509.08 g/mol	599.65 g/mol
Lattice constants (Guinier data)	<i>a</i> = 453.6(1) pm <i>b</i> = 1054.3(3) pm <i>c</i> = 785.3(2) pm <i>V</i> = 0.3756(2) nm ³	<i>a</i> = 444.3(1) pm <i>b</i> = 1031.2(2) pm <i>c</i> = 779.9(2) pm <i>V</i> = 0.3573(2) nm ³	<i>a</i> = 455.9(2) pm <i>b</i> = 1076.4(3) pm <i>c</i> = 755.2(2) pm <i>V</i> = 0.3706(2) nm ³
Calculated density	8.63 g/cm ³	9.46 g/cm ³	10.75 g/cm ³
Crystal size	25 × 40 × 50 μm ³	40 × 40 × 100 μm ³	5 × 40 × 80 μm ³
Absorption correction	Ψ-scan, ellipsoidal	Ψ-scan, ellipsoidal	Ψ-scan, laminar (100)
Transmission ratio (max./min.)	1.40	1.56	6.56
Absorption coefficient <i>F</i> (000)	33.0 mm ⁻¹ 828	43.3 mm ⁻¹ 856	76.5 mm ⁻¹ 988
θ range for data colln.	2° to 40°	2° to 36°	2° to 33°
Range in <i>hkl</i>	0 < <i>h</i> < 8, ±18, ±14	0 < <i>h</i> < 7, ±16, ±12	±6, ±16, -2 < <i>l</i> < 11
Total no. of reflns.	2502	1815	1626
Independent reflns.	673 (<i>R</i> _{int} = 0.0326)	492 (<i>R</i> _{int} = 0.0574)	382 (<i>R</i> _{int} = 0.0316)
Reflns. with <i>I</i> > 2σ(<i>I</i>)	602 (<i>R</i> _{sigma} = 0.0216)	441 (<i>R</i> _{sigma} = 0.0361)	365 (<i>R</i> _{sigma} = 0.0193)
Data/restraints/params.	673/0/16	492/0/16	382/0/16
Goodness-of-fit on <i>F</i> ²	1.123	1.177	1.132
Final <i>R</i> indices [<i>I</i> > 2σ(<i>I</i>)]	<i>R</i> 1 = 0.0197	<i>R</i> 1 = 0.0200	<i>R</i> 1 = 0.0412
<i>R</i> indices (all data)	<i>R</i> 1 = 0.0255, <i>wR</i> 2 = 0.0429	<i>R</i> 1 = 0.0237, <i>wR</i> 2 = 0.0469	<i>R</i> 1 = 0.0428, <i>wR</i> 2 = 0.1288
Extinction coefficient	0.0022(1)	0.0138(4)	0.0036(7)
Largest diff. peak and hole	1.58 and -2.64 e/Å ³	2.38 and -2.14 e/Å ³	5.53 and -6.04 e/Å ³

Table 3. Atomic coordinates and isotropic displacement parameters (pm²) for EuPdIn₂ (1), YbPdIn₂ (2), and YbAuIn₂ (3) (each of space group *Cmcm*; standard deviations are given in parentheses)

Atom	Wyckoff site	<i>X</i>	<i>Y</i>	<i>Z</i>	<i>U</i> _{eq} ^[a]
EuPdIn₂					
Eu	4 <i>c</i>	0	0.06363(3)	1/4	111(1)
Pd	4 <i>c</i>	0	0.78202(4)	1/4	100(1)
In	8 <i>f</i>	0	0.35177(2)	0.05411(3)	101(1)
YbPdIn₂					
Yb	4 <i>c</i>	0	0.06623(3)	1/4	116(1)
Pd	4 <i>c</i>	0	0.78227(5)	1/4	100(1)
In	8 <i>f</i>	0	0.35604(3)	0.05319(4)	100(1)
YbAuIn₂					
Yb	4 <i>c</i>	0	0.07562(8)	1/4	121(4)
Au	4 <i>c</i>	0	0.78901(8)	1/4	109(4)
In	8 <i>f</i>	0	0.3648(1)	0.0509(1)	107(4)

^[a] *U*_{eq} is defined as one-third of the trace of the orthogonalized *U*_{ij} tensor.

Physical Measurements

Magnetic Data: The magnetic susceptibilities of polycrystalline pieces of **1** and **2** were determined with an MPMS SQUID magnetometer (Quantum Design, Inc.) in the temperature range 4.2–300 K, with magnetic flux densities of up to 5.5 T.

Electrical Conductivity: The specific resistivities of **1** and **2** were measured on small irregular shaped blocks using a conventional four-probe technique over the temperature range 4.2–300 K. Cooling and heating curves were identical within the error limits and were reproducible for different samples.

Acknowledgments

We thank Prof. Wolfgang Jeitschko for his interest and support of this work. We are also indebted to Dipl.-Ing. Ute C. Rodewald for the single-crystal data collections, to Klaus Wagner for the EDX analyses, and to Dr. Wolfgang Gerhartz (Degussa AG) for generous gifts of palladium powder and gold wire. Ya. V. G. is indebted to

the DAAD for a research stipend. This work was financially supported by the Deutsche Forschungsgemeinschaft (Po573/1-2) and the Fonds der Chemischen Industrie.

- [1] *Pearson's Handbook of Crystallographic Data for Intermetallic Phases* (Eds.: P. Villars, L. D. Calvert), American Society for Metals, Materials Park, OH 44073, Second Edition, **1991**.
- [2] Ya. M. Kalychak, *J. Alloys Compds.* **1997**, 262–263, 341.
- [3] D. Kußmann, R.-D. Hoffmann, R. Pöttgen, *Z. Anorg. Allg. Chem.* **1998**, 624, 1727.
- [4] R. Pöttgen, A. Lang, R.-D. Hoffmann, R. Müllmann, B. D. Mosel, B. Künnen, G. Kotzyba, *Z. Kristallogr.* **1999**, 214, 143.
- [5] H. Perlitz, A. Westgren, *Ark. Kemi, Mineral. Geol.* **1943**, 16B, 1.
- [6] B. Aronsson, M. Bäckman, S. Rundqvist, *Acta Chem. Scand.* **1960**, 14, 1001.
- [7] L. Pauling, *The Nature of the Chemical Bond and the Structure of Molecules and Crystals*, Cornell University Press, **1960**.
- [8] R. Pöttgen, *J. Mater. Chem.* **1996**, 6, 63.
- [9] R. G. Pearson, *Inorg. Chem.* **1988**, 27, 734.
- [10] J. Donohue, *The Structures of the Elements*, Wiley, New York, **1974**.
- [11] R. Pöttgen, *J. Alloys Compds.* **1995**, 226, 59.
- [12] R. Pöttgen, R.-D. Hoffmann, G. Kotzyba, *Z. Anorg. Allg. Chem.* **1998**, 624, 244.
- [13] R.-D. Hoffmann, R. Pöttgen, G. A. Landrum, R. Dronskowski, B. Künnen, G. Kotzyba, *Z. Anorg. Allg. Chem.*, in press.
- [14] T. Ito, S. Nishigori, I. Hirimitsu, M. Kurisu, *J. Magn. Magn. Mater.* **1998**, 177–181, 1079.
- [15] R. Pöttgen, J. Grin, *Z. Kristallogr.* **1997**, Suppl. 12, 136.
- [16] K. Yvon, W. Jeitschko, E. Parthé, *J. Appl. Crystallogr.* **1977**, 10, 73.
- [17] G. M. Sheldrick, *SHELXS-86, Program for the Solution of Crystal Structures*, University of Göttingen, Germany, **1986**.
- [18] G. M. Sheldrick, *SHELXL-97, Program for the Refinement of Crystal Structures*, University of Göttingen, Germany, **1997**.
- [19] R. Hoffmann, *J. Chem. Phys.* **1963**, 39, 1397.
- [20] R. Hoffmann, *Solids and Surfaces: A Chemist's View of Bonding in Extended Structures*, VCH, Weinheim, New York, **1988**.
- [21] J. H. Ammeter, H.-B. Bürgi, J. C. Thibeault, R. Hoffmann, *J. Am. Chem. Soc.* **1978**, 100, 3686.
- [22] J. P. Desclaux, *At. Data Nucl. Data Tables* **1973**, 12, 311.
- [23] P. Pykkö, L. L. Lohr, Jr., *Inorg. Chem.* **1981**, 20, 1950.
- [24] G. A. Landrum, YAEHMOP (Yet Another Extended Hückel Molecular Orbital Package), Version 2.0, **1997**; available at: <http://overlap.chem.cornell.edu:8080/yaehmop.html>

Received November 16, 1998

[I98394]